RSC Advances

ROYAL SOCIETY OF CHEMISTRY

www.rsc.org/advances

Unraveling the real structures of solution-based and surface-bound poly(3-hexylthiophene) (P3HT) oligomers: a combined theoretical and experimental study

Dalila Khlaifia[1,2], Christopher P Ewels[2], Florian Massuyeau[2],Mourad Chemek[1], Eric Faulques[2], Jean-Luc Duvail[2*], Kamel Alimi[1*]

[1] Unité de Recherche, Matériaux Nouveaux et Dispositifs Electroniques Organiques, Faculté des Sciences de Monastir, University of Monastir, 5000 Monastir, Tunisia

[2] Institut des Matériaux Jean Rouxel, UMR6502 CNRS, Université de Nantes, 2 rue de la Houssinière, F-44322 Nantes, France

* Corresponding authors: Jean-Luc Duvail, Kamel Alimi

Abstract: While the crystalline structure for regio-regular poly(3-hexylthiophene) (P3HT) in thin films is well established, the conformation of P3HT chains in solution has received less attention. Nevertheless, the control of this in-solution structure can be used for managing the structure-processing relationship, a foremost point to improve the optoelectronic behavior and thus the efficiency of devices exploiting electroactive polymers. In the current study, we report a combined theoretical and experimental study of P3HT and a series of oligomers, both in the solid state and in solution. $(3HT)_n$ oligomers were simulated in a variety of planar and non-planar conformations by means of density functional theory (DFT) and time-dependent DFT (TDDFT), comparing results for various functionals with and without dispersion correction in order to evaluate the role of intermediate and long-range effects. Our calculations show that regio-regular P3HT chains adopt a twisted conformation in solution (dihedral angle of about 40°), which contrasts with the well-established planar (θ = 0°) conformation when deposited onto a substrate, due to inter-chain interactions. Determining the Raman spectra, electronic gaps, quasi-particle energies and optical spectra, a good agreement between experimental and simulated optical absorption spectra was obtained for the in-solution case. This study will help to promote the development of alternative strategies for controlling the optoelectronic features of conjugated polymers and polymer blends by exploiting the in-solution structure.

1. Introduction

Thiophene-based polymers with attached alkyl side chains (C_nH_{2n+1}) in the 3-position of the thiophene rings are among the most powerful electroactive polymers in material science, making them very important for various applications in optoelectronics [1-4]. The interest in these conjugated polymers is due to their good solubility [5,6], processability [7,8], and high thermal stability. Additionally it is possible to tune their structural, electronic, optical and transport properties, both via modifying the side chain length, and the type of attachment to the polymer chain to get head-to-head (HH), head-to-tail (HT), tail-to-tail (TT) configurations [9-11]. In particular poly(3-hexylthiophene) (P3HT) has been widely adopted as a hole transporting material in organic electronics, owing to its high drift mobility up to ($0.1 cm^2 V^{-1} s^{-1}$) [12,13]. The physical, chemical and optical properties of a crystalline polymer are strongly influenced by the material morphology and the crystal structure [14]. The control of the regio-regularity leads to P3HT molecules with a highly ordered self-organizing structure through π-π interaction between thiophene rings and weak interaction between alkyl chains, which can strongly improve photoconversion properties [15]. Furthermore, the availability of precisely defined oligomer conformations is useful to control the crystal structure through self-assembly processes and to improve the performance of these materials as an active layer in organic electronic devices. It is important to note that in some cases, P3HT oligomers can even function and perform better than their polymeric counterparts in optoelectronic devices [16]. For this reason, the study of the conformation and the intermolecular interactions between isolated oligomers is of a great interest both in the solution and the solid-state phase.

Various experimental techniques including X-ray diffraction, atomic force microscopy (AFM), and polarized optical microscopy have been used to understand the structure of P3HT [17-22]. However, there remain open questions concerning the morphology of P3HT in solution and in the solid state. Most experimental studies indicate that the P3HT backbone is planar (or almost planar), allowing maximum overlap between π orbitals along first-neighbor backbones [20-23]. By contrast, observations by Bundgaard and Krebs [24] of the shifts in optical absorption (and hence band gap) between polymer in solution and in the solid state suggest that P3HT organizes in different ways in the two cases. Some studies also propose that the presence of alkyl groups can cause local non-planarity, which weaken the π-conjugation along the polymer backbone [25,26]. Therefore, despite the experimental data obtained so far, there is a need for precise structural and optical understanding at the atomic

level of P3HT, notably in the excited state for which very little data exists. Quantum chemical modeling by density functional theory has been used successfully to obtain detailed morphological information for P3HT, such as optimized geometries, electronic structure, frontier molecular orbital energies and vibrational dynamics in model systems. However, there are limitations in modeling the torsional potential of P3HT oligomers, and ground state structures are not always fully structurally unconstrained [27,28].

Additionally, the choice of solvent has been shown to play a central role in the self-crystallinity process and subsequent molecular arrangement, but solvent effects were not included in most calculations published to date [18,29]. No studies have been reported on their excited state structures and properties.

The current study aims first to determine the stable conformation adopted by $(3HT)_n$ oligomers chains, their degree of conjugation and the corresponding photophysical properties, and to compare with experimental optical absorption spectra both in solution (data from [30]) and deposited as thin films. The most stable conformation of isolated regio-regular P3HT oligomers as a function of backbone torsion was explored systematically with and without dispersion. Besides the (B3LYP/6-31G (d)) exchange-correlation functional, which does not include any long-range effects due to electronic interactions between adjacent alkyl chains or between the chains and the thiophene backbone, CAM-B3LYP and WB97X(D) were also used to evaluate the role of the correlated non-covalent interactions. The geometries obtained for the most stable conformations were used as input data for full optimization calculations. Raman and UV-Visible spectra of the resultant P3HT oligomers were then calculated using Density Functional Theory (DFT) and Time-Dependent DFT (TDDFT) respectively, allowing incorporation of the full associated electronic excited state behavior. In parallel, we produced an experimental series of Raman and UV-Vis spectra for P3HT both in chloroform and in thin film. Through comparison of the theory and experiment, we were able to determine the favorable structural configurations of P3HT in both cases.

2. Experimental and Computational details

2.1. Experimental section

Samples were prepared using Sigma Aldrich Regio-regular Poly (3-hexylthiophene) (RR-P3HT) (a regio-regularity HT-HT (head to tail): (head to tail) >99%, an average molecular weight M_w in the range of 15000-45000 g mol^{-1}) and chloroform ($CHCl_3$) (ACS reagent, ≥99.8%, including ethanol as stabilizer). P3HT solution was prepared with a concentration of 1 $mg.mL^{-1}$ under an argon atmosphere in glove box. The obtained solution

was then heated during 5 min in 50°C to achieve a complete dissolution of the P3HT in the solvent. Thin films were deposited by spin coating the solution on quartz substrates.

UV-visible spectra of P3HT thin film and P3HT solution have been measured using a Varian CARY 5 UV-visible-near infrared spectrophotometer with a wavelength range varying from 2000 (0.62 eV) to 200 nm (6.2 eV). Raman spectra with spectral resolution ~2 cm^{-1} were recorded at 785 nm excitation (50× objective) with a Renishaw Raman Microscope, using a laser power of 0.025 mW and an acquisition time of 10s. The homogeneity of the P3HT films was shown by Raman scattering studies for different regions of the film.

2.2. Computational details

The DFT calculations were carried out using Gaussian 09, revision A.02 [31], including the presence of chloroform solvent, on a SGI origin 2000 server. Molecular geometries were fully optimized using Becke's three-parameter Lee-Yang-Parr exchange-correlation functional (B3LYP) with the 6-31G (d) basis set. The choice of the basis set follows previous studies, for example by Roas et al [32] who demonstrated its validity for conjugated thiophene systems. No initial symmetry constraints were applied. The B3LYP level of theory is frequently used for calculating the orbital energy levels of monomeric and oligomeric model structures to approximate conjugated infinite polymers. Additionally, it can permit to reproduce the charge transfer in the case of conjugated polymers [33,34]. However, it does not include any long-range effects due to electronic interactions between adjacent alkyl chains, or between the chains and the thiophene backbone [35]. Thus it possibly overestimates the energy between fully delocalized (planar) and highly twisted forms, consequently overstabilizing the planar structure of conjugated molecules [36]. So, CAM-B3LYP and WB97X(D), used successfully for evaluating torsional potential of alkyl, donor, and acceptor substituted bithiophene [37], were also used to evaluate the role of the correlated non-covalent interactions on the overall structural conformation. The torsional potential energy and the energy gap calculated for the different DFT variants are discussed in Section 3.5 below with detailed results in Supplementary Materials.

We first performed a conformational search on the torsional potential of the various P3HT oligomers. In each case, the ground-state geometry of the oligomer was determined in the gas phase at a fixed angle θ between adjacent thiophene rings, where θ is defined as the dihedral angle S-C-C-C along the backbone (Figure 1). The most stable geometries of the oligomers were then reoptimized in gas-phase and in the presence of chloroform (applied via a continuum solvent model) without any constraint, prior to simulating Raman intensities and optical properties.

Detailed knowledge of the energy gap in π-conjugated polymers and especially in poly (alkyl-thiophenes) is highly important for eventual applications [27-29]. Here, two approaches have been used to evaluate the energy gaps of the P3HT oligomers. The energy gaps have been estimated from the ground state via the energy difference E_g^{HL} between the highest occupied orbital (HOMO) and the lowest unoccupied molecular orbital (LUMO). The optical band gap E_g^{opt} is defined as $E_g^{opt} = E(S_1) - E(S_0)$. E_g^{opt} and oscillator strengths of each P3HT oligomer were determined from the ground state optimized geometries in chloroform solution, using TDDFT with a B3LYP/6-31G (d) level [38]. Finally the energy gaps for the infinite chain were extrapolated from the finite oligomer using a Kuhn fit, which has been successfully employed to investigate energy gaps for different infinite polymer chains [39-41]. Using the resulting ground state optimized geometries in chloroform solution, TDDFT [41] calculations of the E_g^{opt} and the oscillator strengths of each P3HT oligomers were performed. It can be noticed that McCormick et al [42] have shown that B3LYP is reliable to evaluate the HOMO-LUMO energy gap, based on a series of TDDFT calculations for twenty two different conjugated polymers by comparing the frontier orbital energies obtained with different functionals.

3. Results and discussion

3.1. Structural conformation of P3HT oligomers

The model structure is defined in Figure 1 for a n-unit oligomer, requiring n-1 inter-ring torsional angles θ. The torsional angle θ along the backbone was determined from the C-C-C-S bonds marked in red. Conformational analysis of P3HT oligomers was performed by varying the torsional angle θ between each pair of adjacent rings, scanned with 10° steps between the cis (θ=0°) and the trans conformation (θ=180°). For each conformation, the torsional angle was held fixed while the other structural parameters were optimized without constraint.

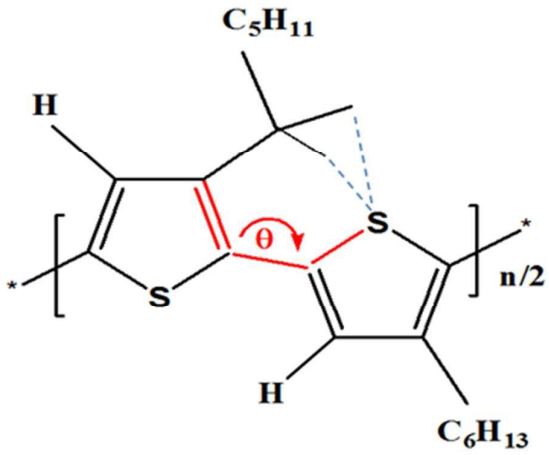

Figure 1. Schematic representation of the P3HT dimer. The angle θ is the central torsional angle along conjugated skeleton determined from the C-C-C-S bonds marked in red.

The resultant curves of potential energy for the P3HT oligomers are shown in Figure 2(a). For each oligomer, the energy difference is quoted relative to the corresponding absolute minimum conformation divided by the number of monomer ($(E_n(\theta) - E_n(40°))/n$). All the structures give two energy minima at about θ=40° and 135°, with the overall minimum at 40°. For longer chain lengths, a local minimum appears at 180°, while in all cases the planar 0° structures represent a local maximum. The torsional profiles showed three maxima situated at θ=90°, 170° and 0° with the overall maximum at 90° that results from breaking of the conjugation between the rings and from the poor intramolecular charge carrier mobility. The torsional potential profiles are in good agreement with the hypothesis suggested by Cui and Kertesz [43,44] using semi-empirical approaches. Indeed, in their calculations on poly(3-alkylthiophenes), they have predicted that, due to the repulsion between the sulfur atom and the adjacent methylene (see Figure 1), isolated poly(3-alkylthiophene) should adopt a non-planar chain conformation with torsion angles at about 40°. It can be noted that very similar angular dependence are found for calculations with CAM-B3LYP and WB97X(D) functionals (see Figure S1).

In order to illustrate the charge distribution of P3HT, the frontier molecular orbitals (HOMO and LUMO) are shown on Figure 2(b) both in the twisted (θ=40°) and in the planar (θ=0°) conformations of $(3HT)_8$. It is important to note that the frontier orbitals are slightly dependent on the torsion angle θ in the range of 0°-40° and that the side alkyl chains do not play a role in the charges distribution.

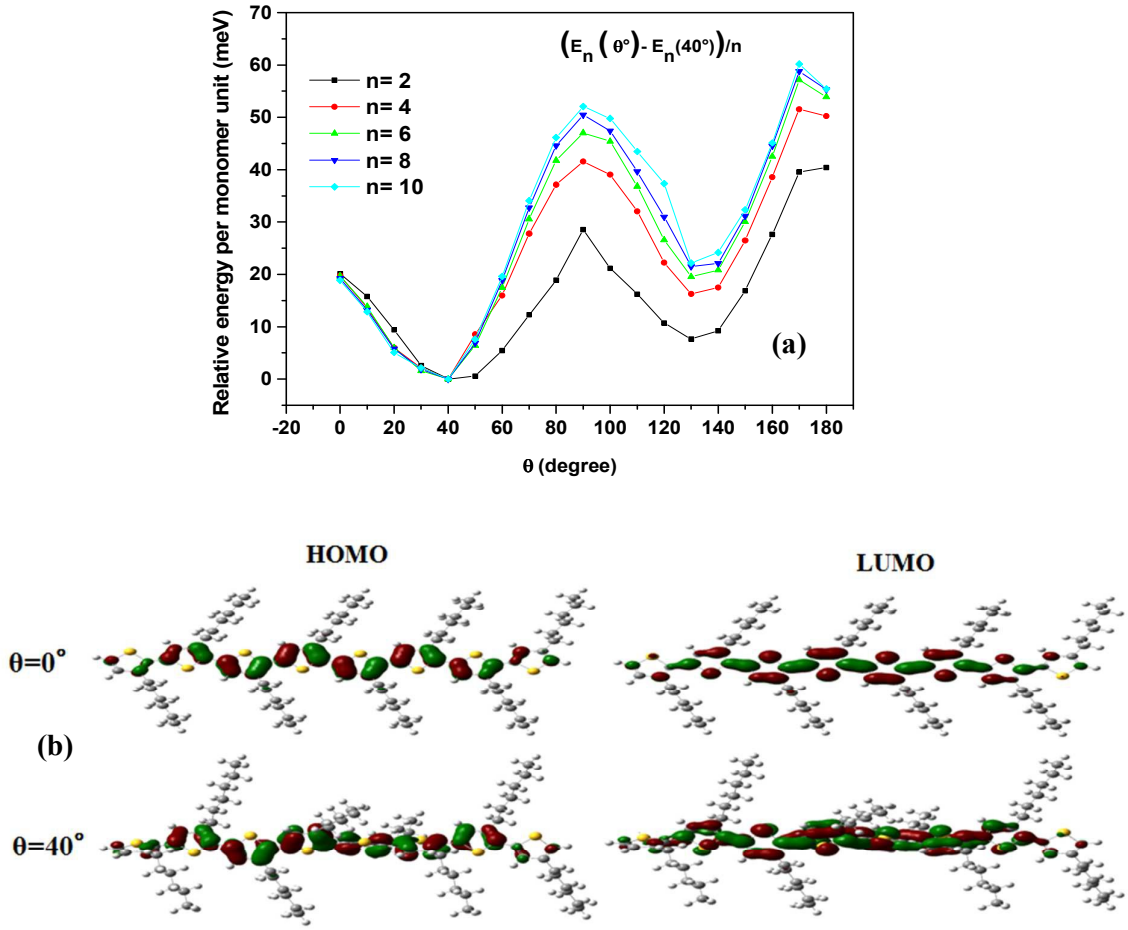

Figure 2. Torsional potential energy per monomer curves of P3HT oligomers in vacuum containing two to ten monomer units as a function of the inter-ring torsional angle θ (a). HOMO and LUMO orbitals for the planar (θ=0°) and twisted (θ=40°) structures of $(3HT)_8$ (b).

3.2. Energy gaps

The energy diagram in Figure 3 presents the different energy levels and energy values in a conjugated polymer in its ground and excited state. We examine first the calculated HOMO-LUMO gaps (E_g^{HL}) of the P3HT oligomers as a function of the inverse of monomer number. E_g^{HL} is the lowest electronic excitation energy possible in a system. Depending on the functional used, large discrepancies are evidenced (Figure S2). While B3LYP predicts E_g^{HL} close to the experimental value, both CAM-B3LYP and WB97X(D) significantly overestimate E_g^{HL}. This result motivates our choice of using B3LYP for examining the ground state of P3HT oligomers. It is emphasized that the HOMO-LUMO extrapolated gap for the infinite chain in the cis-planar (θ=0°) conformation (about 2.02 eV) is

in quite good agreement with electronic band gap of P3HT thin film, when the planar conformation results from inter-chain interactions not included in our calculations. We next estimate the values of energy gaps of the system, as defined in Figure 3. E_0 is the total energy of the neutral system having *n* electrons in its ground state. The electronic energies gaps of the P3HT oligomers can be estimated in three ways as proposed in [29].The first one is the energy difference between HOMO and LUMO E_g^{HL}. The fundamental energy E_g^{fund} is the difference between the vertical ionization potential and electron affinity, calculated as the energy difference between the neutral and the ionic states of each system. Hence, the $IP = E(+1) - E_0$ ($EA = E_0 - E(-1)$) is calculated as the energy difference between the neutral and the cationic (+1) (anionic (-1)) species respectively [45,46]. The lowest excited energy E_g^{opt} is the energy of the transition from the ground state (S_0) to the first excited state (S_1) calculated by TDDFT.

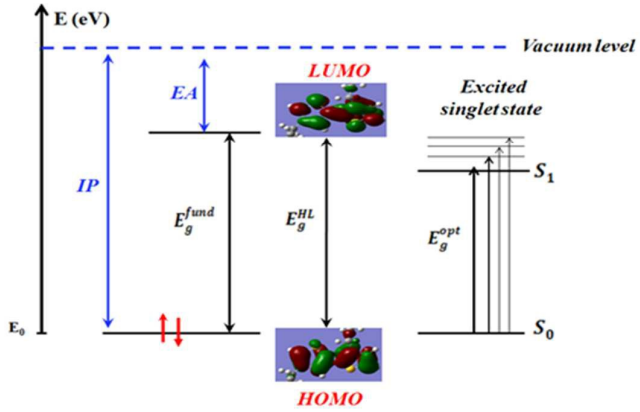

Figure 3. Energy diagram in a conjugated polymer in its ground and excited state.

3.3. HOMO-LUMO and the lowest excitation energy gaps

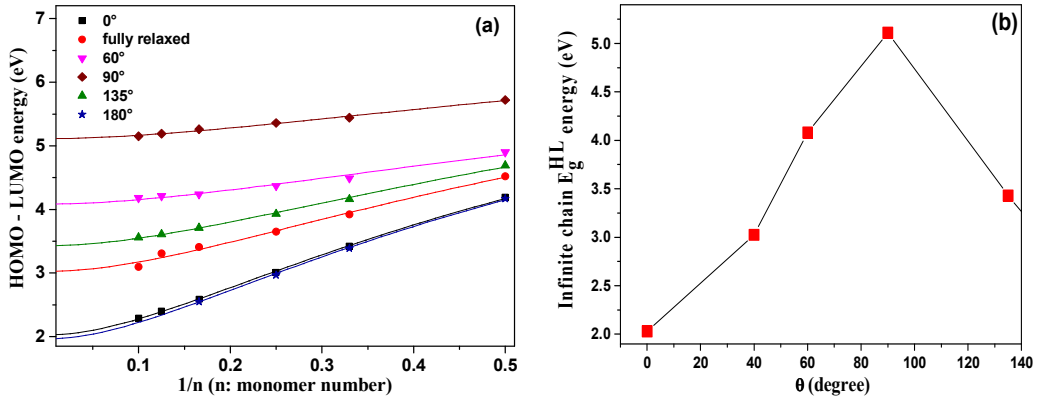

Figure 4. B3LYP HOMO-LUMO gaps (E_g^{HL}) of the P3HT oligomers as a function of the inverse of monomer number and the torsional angle between the thiophene units (the dihedral angle was fixed at θ= 0°, 60°, 90°, 135°,while the most stable structure was fully relaxed: θ ≈ 37° to 41° depending on n) (a). Extrapolated gaps for the infinite chain by Kuhn fit method (b).

HOMO-LUMO energy gap of P3HT oligomers (eV)	E_g^{HL} (eV) θ = 40°	E_g^{HL} fully relaxed (eV) (average angle)	E_g^{HL} (eV) θ = 0°
n=2	4.54	4.52 (38.9°)	4.19
n=3	3.95	3.92 (39.4°)	3.42
n=4	3.70	3.65 (40.2°)	3.01
n=6	3.44	3.41 (41.4°)	2.59
n=8	3.33	3.31 (40.5°)	2.40
n=10	3.27	3.09 (37.3°)	2.29

Table.1. E_g^{HL} energy gap (eV) of $(3HT)_{n=2\ to\ 10}$ oligomers in their planar (θ=0°), twisted (θ=40°) and reoptimized fully relaxed conformations (value of the average θ angle along the backbone) calculated with DFT/B3LYP-6-31G (d), all calculated in gas phase.

The Figure 4(a) shows the variation of E_g^{HL} energy gap with the oligomer length and the dihedral angle θ in the gas phase. Detailed values are reported in Table 1. Whatever the θ value, a decrease of the HOMO-LUMO gap is obtained when the length of the chain increases, but this decrease is larger when the conformation tends toward the planar one. It is thus related to the sp^2-sp^2 interaction promoting a planar. Another important result is the dependence of the overall energies with the degree of planarity. It is particularly illustrated by the E_g^{HL} values for different θ angles extrapolated to the case of the infinite chains, as reported in Figure 4(b). Such values were obtained by application of the Kuhn fit method [39] to extrapolate the gap dependence out to longer systems, i.e. infinite chains. It can be noted that for θ=180°, long chains would result in a coiling configuration with overlapping of alkyl chains, which is not relevant. As the torsion angle θ shifts away from the planarity case, the HOMO-LUMO energy displays a strong destabilizing trend. The variation in extrapolated infinite HOMO-LUMO gap with torsional angle agrees with the energetic variation shown in Figure 2, except for θ=0°, as expected when the structural stability is balanced by the degree of π-conjugation of the polymer backbone. The conjugation is strongly dependent on the degree of overlap of neighboring π-orbitals between thiophene units, which can be affected in three ways: C-C bond elongation, flexion of the backbone axis, and torsion. We have fixed the torsion, and it shows by far the most important variation. In the case of short chain length

(n < 8) for θ =180°, there is a much increased π-π overlap compared to θ =135°, thus resulting in an increased conjugation and a lower gap.

The comparison of the HOMO-LUMO extrapolated gap values for the infinite P3HT chain with the experimental values gives useful indication. The electronic band gap values of RR-P3HT thin film measured experimentally are in the range 1.9-2.1eV [47-49]. The simulated value for the cis-planar E_g^{HL}(θ=0°)≈ 2 eV is in excellent agreement with these experimental values, while there is a large discrepancy with the twisted conformation E_g^{HL} (θ=40°)≈ 3 eV. It suggests that the complexity of the local structure of P3HT when processed in thin films can be partly apprehended from the ideal simulated structures. This point is further discussed and confirmed later, while comparing simulated and experimental optical absorption and Raman spectra.

Considering the value of the average θ angle along the backbone in the fully relaxed conformation, it can be noted (Table 1) that it varies slightly with the number n of monomers, with a shift smaller than 3°. Then, the 40° conformation can be considered close to the relaxed one and it has been used for further investigations.

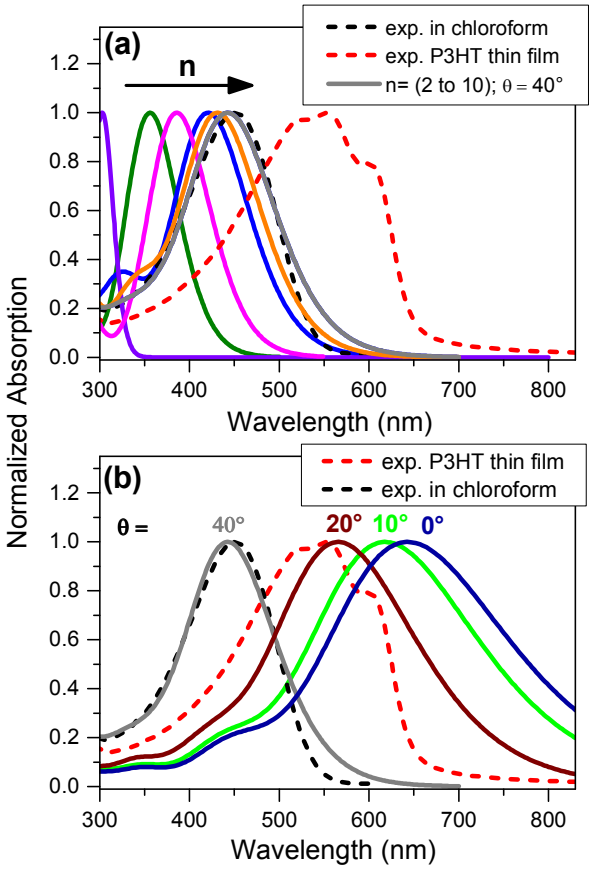

Figure 5. Optical absorption spectra. (a) Comparison of simulated spectra of the $(3HT)_n$ oligomers in the conformation fixed at θ = 40° (n = 2: violet; 3:olive; 4: pink; 6: blue; 8: orange; 10: gray) with experimental spectra in chloroform (dashed black) and in thin film (dashed red). (b) Comparison of experimental P3HT spectra in chloroform (dashed black) and in thin film (dashed red) with simulated spectra for n = 10 at different constrained angles: θ=40° (gray), θ=20° (wine), θ=10° (green) and θ=0° (blue).

Oligomer	Conformation	Experimental Optical gap (eV)[30]	TD-DFT		
			E_g^{opt}(eV)	μ (D)	f
2	40°	**4.12**	4.10	33.1	0.45
	0°		3.83	31.0	0.50
3	40°	**3.62**	3.48	28.1	0.73
	0°		3.08	24.8	0.86
4	40°	**3.33**	3.21	25.9	1.02
	0°		2.67	21.5	1.28
5	40°	**3.18**	3.05	24.6	1.28
	0°		2.41	19.4	1.66
6	40°	**3.06**	2.94	23.7	1.55
	0°		2.24	18.0	2.04
7	40°	-	2.87	23.1	1.83
	0°		2.12	17.1	2.40
8	40°	**2.94**	2.83	22.8	2.11
	0°		2.03	16.4	2.75
10	40°	**2.88**	2.80	22.4	2.70
	0°		1.93	15.5	3.43

Table 2. TDDFT optical energies $\boldsymbol{E_g^{opt}}$ (in eV), transition dipole moments (μ), and oscillator strength (f) from the ground state to the first excited state ($S_0 \rightarrow S_1$) of P3HT oligomers simulated in chloroform for 0° and 40° conformations. The experimental optical gaps of the corresponding oligomers in the same solvent are taken from reference [30].

Figure 5(a) and Figure 5(b) depict the experimental and simulated optical properties of selected P3HT oligomers in twisted and planar conformations. All the simulated spectra of twisted oligomers show a shift towards longer wavelengths when the oligomer length increases (Figure 5(a)). Table 2 compiles the values of the calculated optical gap, the transition dipole moment and the oscillator strength of the lowest excited states of the oligomeric structures of P3HT for the two conformations, as well as the corresponding experimental optical gaps. The optical energy E_g^{opt} deduced from the transition between the

ground state (S_0) and the first excited state (S_1) decreases on going from the shorter to the longer oligomers. As discussed previously, such an effect is attributed to the increase of the conjugation length when the number of monomer increases. It is emphasized that the absorption maximum at 442 nm for the n=10 monomer units at θ=40° is close to the experimental absorption maximum $\lambda_{\max}(P3HT) = 451$ nm in chloroform. The calculated values of E_g^{opt} for n = 2 to 10 are also in very good agreement with experimental results obtained by Koch et al. (Table 2, [30]), who performed UV-Vis measurement of a series of thirty-six P3HT oligomers in chloroform. When switching from solution to solid state in a thin film oligomer configuration, a redshift of about 100 nm is experimentally measured, as shown in Figure 5(b). This red shift can be attributed to an increase of the conjugation length of the P3HT molecules, which results from the supramolecular ordering. Indeed, P3HT film self-organizes due to both π-π stacking between conjugated backbones and interactions between alkyl chains, which promote polycrystalline domains with polymer chains orientated in two dimensional lamellar structures. The conjugation length in the crystalline domains is larger because the polymer molecules are well-oriented.

The UV-Vis spectrum of P3HT film exhibits three bands around 2.02 (612 nm), 2.25 (551 nm) and 2.42 eV (512 nm). The band around 2.02 eV is assigned to the 0-0 transition of H-aggregates of regio-regular P3HT [50]. It is dependent on the regio-regularity of the polymer and thus on the local ordering of the packing structure and aggregation. The higher-energy band is usually attributed to more disordered chains [50-51]. Indeed, a real thin film includes a local disorder related for example to grain boundaries between well-ordered grains, or to local fluctuation of the inter-chain distance. It can result in some deviations to the planarity of the chain, i.e. θ torsional angle different from 0°. This more complex structure in real systems is reflected by the broadening of the experimental optical absorption spectrum. This interpretation is supported by our calculations, as shown in Figure 5(b) where simulated optical absorption spectra of n= 10 oligomer for θ=0 °, 10 °, 20 ° and 40° in chloroform are compared with the experimental spectra of P3HT in the solution and in the solid state. It is highlighted that the experimental absorption maximum in the thin film is located close of the calculated absorption maximum for the n=10 oligomers at θ=20° (566 nm). This agrees with our previous analysis that in solid films, polymer chains may adopt conformations with a small dihedral angle distribution.

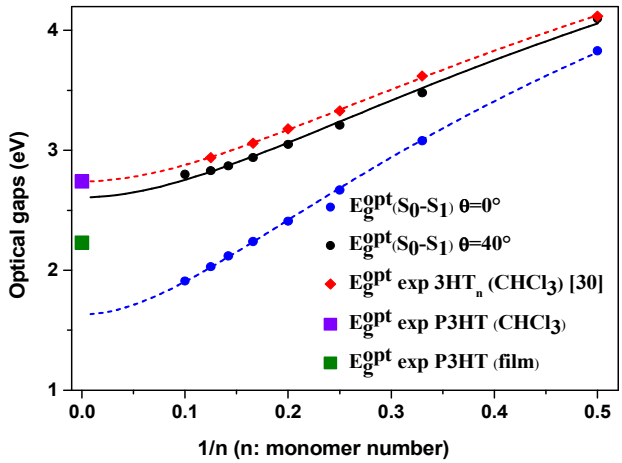

Figure 6. Calculated energy gaps E_g^{opt} of P3HT oligomers in their twisted conformations (θ=40°, black circles) and planar conformations (θ=0°, blue circles) as a function of reciprocal chain length. The red diamond symbols show the experimental band gaps E_g^{opt} of $(3HT)_n$ oligomers in chloroform, taken from ref [30] (dotted red line). The corresponding lines show the fits of these values, extrapolated for the infinite chain by Kuhn fit method. The violet and green full square symbols show the measured band gap E_g^{opt} of P3HT ("infinite" chain length) in chloroform and thin film, respectively.

Such an analysis is also supported by Figure 6, which shows the variation of energy gaps of the P3HT oligomers versus $1/n$ in both planar (θ=0°) and twisted (θ=40°) conformations. These are compared to the experimental gap $E_g^{opt} = E(S_0 - S_1)$ of the corresponding oligomers in solution, as taken from reference [30] and those of P3HT measured in solution ($CHCl_3$) and in thin film. To estimate the polymers band gap for the two conformations of the oligomers, the approach reported by Kuhn was used. Using this extrapolation $E_g^{opt} = E(S_0 - S_1)$ is estimated to be 1.65 eV and 2.67 eV for an infinite planar or 40°-twisted conformation, respectively. For the same reasons discussed above for the optical absorption spectra, there is a good agreement between calculation and experiment for the solution case, while a significant discrepancy is observed for the thin film case.

To summarize, the optical absorption experimental and calculated spectra are consistent with a picture where by the oligomer chains in solution are twisted with backbone torsion near 40°, but are increasingly aligned towards 0° torsion upon thin film deposition.

3.4. Simulated vibrational spectra

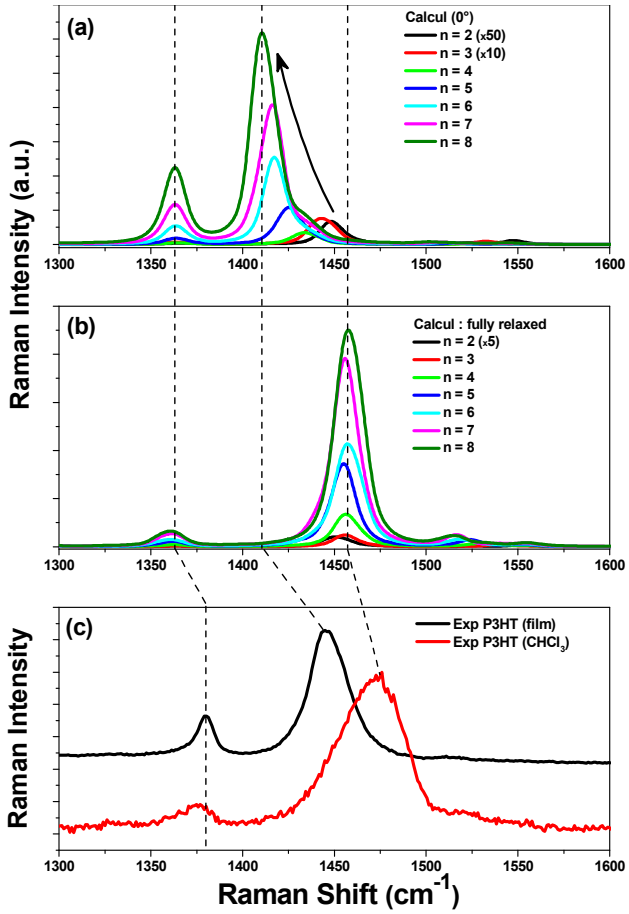

Figure 7. Comparison of simulated and experimental Raman spectra of P3HT oligomers and polymers. Simulated Raman spectra in the planar (θ = 0°) (a) and in the fully relaxed conformation (θ≈ 37° to 42° depending on n) (b) as a function of the chain length (n= 2 to 8 monomer units). Calculated Raman shifts are scaled by an empirical factor of 0.96 [54]. Experimental Raman spectrum (λ_{exc} = 785 nm) of a P3HT thin film and P3HT in $CHCl_3$ (c).

Based on the fully optimized structure of P3HT oligomers (n=2 to n=8) in the neutral ground state, simulated Raman spectra are calculated using DFT/B3LYP/6-31G (d). Previous work has shown that B3LYP/6-31G (d) can reproduce observed experimental Raman spectra of organic materials with good accuracy [52-54]. Recently, Baggioli et al have shown that a full-length alkyl fragment can influence significantly the optoelectronic properties of alkylthiophene-based polymers [55].

In this part, we calculate Raman spectra of geometrically optimized P3HT oligomers (i.e. full alkyl side chains) with 2 to 8 units in the more stable conformation. Starting from the

40° structure, oligomers were allowed to relax in order to get the more stable conformation and the corresponding Raman spectrum. It results in small changes in the dihedral angles depending on the n value. For example, the average dihedral angle θ along the oligomers is about 40.5° in the case n = 8. The effects of the conjugated oligomer length on the vibrational modes were investigated. Figure 7(a) shows the simulated Raman spectra of the normal modes of P3HT oligomers. All the presented calculated Raman shifts were scaled by an empirical factor of 0.96 for a set of comparison with experimental spectra [54]. Various Raman modes are obtained between 600 and 1700 cm^{-1}, with the main in-plane ring skeleton modes in the range of 1300-1600 cm^{-1}, showing the symmetric C=C stretching and the C-C intra-ring stretching modes characteristic of P3HT oligomers and polymer the C-H bending mode with the C-C inter-ring stretching mode at ~1170 cm^{-1}[52,56]. The most intense band associated to the double bonding C=C stretching mode exhibits a large downshift when the chain length increases (Figure 7(a)): 1449 cm^{-1} for $(3HT)_2$, 1435 cm^{-1} for $(3HT)_4$, 1425 cm^{-1} for $(3HT)_5$, 1417 cm^{-1} for $(3HT)_6$ and 1410 cm^{-1} for $(3HT)_8$. The C=C band intensity strongly increases when the backbone length increases. These two effects are commonly attributed to the increase of the conjugation along the skeleton when the chain length increases. However, the strong variation of the position of the C=C stretch band as a function of the chain length in the planar case (Figure 7(a)) strongly contrasts with the almost unchanged position at about 1455 cm^{-1} for the fully relaxed conformation (θ≈ 37 to 41° depending on n) shown Figure 7(b). This result can be explained since the non-linearity of the backbone in the relaxed conformation restricts the conjugation extension along the backbone. Additionally, the weaker Raman line at ~1365 cm^{-1} for both the planar and fully relaxed conformation is attributed to a single bonding C-C stretch mode. It doesn't show any significant Raman shift with the increase of the chain length, but a concomitant increase of the intensity with the backbone length. Similar results were reported for the Raman spectra simulations of 3 to 7 thiophene units by Tsoi and coworkers [52], with a shift limited to 5 cm^{-1} for the C-C band while the downshift of the C=C band reaches 25 cm^{-1}.

Finally, it is interesting to compare the simulated spectra with the experimental ones for P3HT in-solution or in solid state reported in Figure 7(c). The C-C stretch mode is located at ~1375 cm^{-1} in both cases, supporting the simulations of Figure 7(a) and Figure 7(b) where the same location is found whatever the conformation. This mode is not a collective one, as its location doesn't change with the chain length (i.e. the conjugation length), whatever the conformation [57]. For the C=C stretch band, it is located at 1445 cm^{-1} and at 1475 cm^{-1} for the film and the in-solution case, respectively. It can be noted that this mode has been measured at 1475 cm^{-1}

for $(3HT)_8$ in chloroform [57], showing the same Raman feature for the polymer and this octamer. This redshift by 30 cm^{-1} is significantly smaller than the maximum 45 cm^{-1} shift calculated between the planar and the fully relaxed conformation. Such a redshift was also calculated by L. Brambilla et al. for $(3HT)_8$ between a planar structure and the fully relaxed one. It can be attributed to the conjugation length distribution in the experimental system and/or to local minor variations in the torsional angle, i.e. to structural deviation from planarity. This point has been well addressed by the investigation of different structures of $(3HT)_8$ (provided by F.P. Koch and P. Smith) by Raman and IR spectroscopy [57].

As deduced from the above study of experimental and calculated optical absorption spectra, the Raman study is consistent with a picture where by the oligomer chains in solution are twisted with backbone torsion close to 40°, but are increasingly aligned towards 0° torsion upon the thin film deposition.

3.5 Choice of exchange-correlation functional

The hybrid-exchange functional B3LYP used in the current study has, for some time, been the standard choice for modeling organic systems such as presented here. Notably it has been shown to give qualitative accuracy in modeling the torsional potential for poly(3-alkylthiophenes) [28,29]. However there are now alternative exchange-correlation functionals available such as CAM-B3LYP and WB97X(D) which overcome some of the limitations of B3LYP, notably through inclusion of empirical dispersion forces. These have been shown to give better quantitative accuracy in structural studies of torsion in [35]. For this reason we compared these three functionals for the P3HT system. The torsional potential energy per monomer for P3HT oligomers containing 2 to 10 monomers units as a function of the inter-ring torsional angle θ (equivalent of Figure 2) is shown in Supplementary Materials Figure S1. As can be seen, there is good qualitative matching between the three functionals, all identifying the same global and secondary minima, suggesting that dispersion effects are minor. Notably B3LYP, CAM-B3LYP and WB97X(D) give approximately the same torsional angle for the ground state structure of 40°. The only differences are in the barrier heights for torsional rotation of the P3HT backbone.

However when we examine the calculated HOMO-LUMO gaps (E_g^{HL}) of the P3HT oligomers as a function of the inverse of monomer number (equivalent of Figure 6), there are large discrepancies between the three functionals (Figure S2). While B3LYP predicts

E_g^{HL} close to experiment, both CAM-B3LYP and WB97X(D) significantly overestimate E_g^{HL}. These results justify our choice of using B3LYP for the current study.

4. Conclusions

In this work, we have performed a combined theoretical and experimental study of conformational preferences of P3HT in thin film and in solution. The conformations preferentially adopted by P3HT oligomers chains were determined from calculations by a detailed investigation of the structural, energetic and spectroscopic characteristics of P3HT oligomer (up to the decamer). This allows a clear identification of the structure-property relationship for 3HT oligomers and P3HT both in solvent and in thin films. For the fully relaxed case (θ≈40° conformation), there is a very good agreement between the experimental and calculated optical spectra for the longer oligomer, with values of E_g^{opt} extrapolated for an infinite chain equal to 2.67 eV. It indicates that in solution, this twisted backbone is the main configuration, whether the functional used includes dispersion corrections (CAM-B3LYP, WB97X(D)) or not (B3LYP). On the contrary, the overestimation of the optical spectrum redshift for the planar case was explained by the discrepancy between the ideal planar conformation of the simulated structures and the real structure of P3HT in thin films including local disorder and interaction between neighbouring P3HT species in crystal packing -which are not considered in our calculations. These results are of great interest for resolving the ambiguity in the literature concerning the structure of P3HT. Beyond the new insight in this relationship, this study may contribute to motivate alternative processing strategies by exploiting the in-solution structure to modify the optoelectronic features of conjugated polymers and polymer blends.

Acknowledgements:

The authors thank J. Y. Mevellec and N. Stephant for their help in Raman spectroscopy studies and SEM characterization, respectively. We thank the CCIPL, “Centre de Calcul Intensif de Pays de la Loire”, where these calculations were performed.

References

1 G. Xiao, Y. Guo, Y. Lin, X. Ma, Z. Su and Q. Wang, *Phys. Chem. Chem. Phys.*, 2012, **14**, 16286–16293.

2 Y.-J. Cheng, S.-H. Yang and C.-S. Hsu, *Chem. Rev.*, 2009, **109**, 5868–5923.

3 F. Liu, Y. Gu, J. W. Jung, W. H. Jo and T. P. Russell, *J. Polym. Sci. Part B: Polym. Phys.*, 2012, **50**, 1018–1044.

4 S. Grigorian, D. Tranchida, D. Ksenzov, F. Schäfers, H. Schönherr and U. Pietsch, *Eur. Polym. J.,* 2011, **47**, 2189–2196.

5 M. C. Iovu, R. Zhang, J. R. Cooper, D. M. Smilgies, A. E. Javier, E. E. Sheina, T. Kowalewski and R. D. McCullough, *Macromol. Rapid. Commun.*, 2007, **28**, 1816–1824.

6 G. Barbarella, A. Bongini and M. Zambianchi, *Macromolecules*, 1994, **27**, 3039–3045.

7 S. Hotta, S. Rughooputh, A. J. Heeger and F. Wudl, *Macromolecules*, 1987, **20**, 212–215.

8 F. P. V. Koch, P. Smith and M. Heeney, *J. Am. Chem. Soc.*, 2013, **135**, 13695–13698.

9 R. D. McCullough and S. P. Williams, *J. Am. Chem. Soc.*, 1993, **115**, 11608–11609.

10 M. A. de Oliveira, W. B. de Almeida and H. F. dos Santos, *J. Braz. Chem. Soc.*, 2004, **15**, 832–838.

11 M. Skompska and A. Szkurlat, *Electrochim. Acta*, 2001, **46**, 4007–4015.

12 H. Wei, L. Scudiero and H. Eilers, *Appl. Surf. Sci.*, 2009, **255**, 8593–8597.

13 D. L. Cheung, D. P. McMahon and A. Troisi, *J. Phys. Chem. B.*, 2009, **113**, 9393–9401.

14 P. C. Ewbank, M. C. Stefan, G. Sauvé and R. D. McCullough, *Handbook of Thiophene-Based Materials: Applications in Organic Electronics and Photonics, 2 Volume Set*, 2009, 157.

15 Y. Takizawa, T. Shimomura and T. Miura, *J. Phys. Chem. B.*, 2013, **117**, 6282–6289.

16 J. E. Hernandez, H. Ahn and J. E. Whitten, *J. Phys. Chem. B.*, 2001, **105**, 8339–8344.

17 Z. Wu, A. Petzold, T. Henze, T. Thurn-Albrecht, R. H. Lohwasser, M. Sommer and M. Thelakkat, *Macromolecules*, 2010, **43**, 4646–4653.

18 S. Ko, E. T. Hoke, L. Pandey, S. Hong, R. Mondal, C. Risko, Y. Yi, R. Noriega, M. D. McGehee, J.-L. Brédas, A. Salleo and Z. Bao, *J. Am. Chem. Soc.*, 2012, **134**, 5222–5232.

19 M. Chemek, D. Khlaifia, F. Massuyeau, J. L. Duvail, E. Faulques, J. Wéry and K. Alimi, *Synth. Met.*, 2014, **197**, 246–251.

20 R. Colle, G. Grosso, A. Ronzani and C. M. Zicovich-Wilson, *Phys. Status Solidi B*, 2011, **248**, 1360–1368.

21 D. Dudenko, A. Kiersnowski, J. Shu, W. Pisula, D. Sebastiani, H. W. Spiess and M. R. Hansen, *Angew. Chem. Int. Ed.*, 2012, **51**, 11068–11072.

22 R. P. Kurta, L. Grodd, E. Mikayelyan, O. Y. Gorobtsov, I. A. Zaluzhnyy, I. Fratoddi, I. Venditti, M. V. Russo, M. Sprung, I. A. Vartanyants et al., *Phys. Chem. Chem. Phys.*, 2015, **17**, 7404–7410.

23 K. D. Kim, S. Park, S. Nho, G. Baek and S. Cho, *Curr. Appl. Phys.*, 2014, **14**, 1369–1373.

24 E. Bundgaard and F. C. Krebs, *Sol. Energy Mater. Sol. Cells*, 2007, **91**, 954–985.

25 S. M. Bouzzine, S. Bouzakraoui, M. Hamidi, M. Bouachrine, *Asian J. Chem.*, 2007, **19**, 1651-1657.

26 H. Mao, B. Xu and S. Holdcroft, *Macromolecules*, 1993, **26**, 1163–1169.

27 S. B. Darling, *J. Phys. Chem. B.*, 2008, **112**, 8891–8895.

28 R. S. Bhatta, Y. Y. Yimer, M. Tsige and D. S. Perry, *Comput. Theor. Chem.*, 2012, **995**, 36–42.

29 R. S. Bhatta and M. Tsige, *Polymer*, 2014, **55**, 2667–2672.

30 F. P. V. Koch, Dissertation N°20912 ETH Zurich, 2013.

31 M. J. Frisch, G. W. Trucks, H. B. Schlegel, G. E. Scuseria, M. A. Robb, J. R. Cheeseman, G. Scalmani, V. Barone, B. Mennucci, G. A. Petersson, H. Nakatsuji, M. Caricato, X. Li, H. P. Hratchian, A. F. Izmaylov, J. Bloino, G. Zheng, J. L. Sonnenberg, M. Hada, M. Ehara, K. Toyota, R. Fukuda, J. Hasegawa, M. Ishida, T. Nakajima, Y. Honda, O. Kitao, H. Nakai, T. Vreven, J. A. Montgomery and J. E. P. Jr., F. Ogliaro, M. Bearpark, J. J. Heyd, E. Brothers, K. N. Kudin, V. N. Staroverov, R. Kobayashi, J. Normand, K. Raghavachari, A. Rendell, J. C. Burant, S. S. Iyengar, J. Tomasi, M. Cossi, N. Rega, J. M. Millam, M. Klene, J. E. Knox, J. B. Cross, V. Bakken, C. Adamo, J. Jaramillo, R. Gomperts, R. E. Stratmann, O. Yazyev, A. J. Austin, R. Cammi, C. Pomelli, J. W. Ochterski, R. L. Martin, K. Morokuma, V. G. Zakrzewski, G. A. Voth, P. Salvador, J. J. Dannenberg, S. Dapprich, A. D. Daniels, O. Farkas, J. B. Foresman, J. V. Ortiz, J. Cioslowski, D. J. Fox, Gaussian 09, Revision A.02, Gaussian, Inc., Wallingford CT, 2009.

32 G. Raos, A. Famulari and V. Marcon, *Chem. Phys. Lett.*, 2003, **379**, 364–372.

33 D. M. Hinkens, Q. Chen, M. K. Siddiki, D. Gosztola, M. A. Tapsak, Q. Qiao, M. Jeffries-EL and S. B. Darling, *Polymer*, 2013, **54**, 3510–3520.

34 Y. Li and J. B. Lagowski, *Polymer*, 2011, **52**, 4841–4850.

35 A. Dreuw, *Chem. Rev.*, 2005, **105**, 4009−4037.

36 A. Karpfen, *J. Phys. Chem. A.,*1997**, 101***,* 7426-7433.

37 T-J. Lin, S-T. Lin, *Phys. Chem. Chem. Phys.,* 2015, **17**, 4127.

38 E. Runge and E. K. U. Gross, *Phys. Rev. Lett.*, 1984, **52**, 997–1000.

39 J. Torras, J. Casanovas and C. Alemán, *J. Phys. Chem. A.*, 2012, **116**, 7571–7583.

40 S. S. Zade and M. Bendikov, *Org. Lett.*, 2006, **8**, 5243–5246.

41 J. Gierschner, J. Cornil and H.-J. Egelhaaf, *Adv. Mater.*, 2007, **19**, 173–191.

42 T. M. McCormick, C. R. Bridges, E. I. Carrera, P. M. DiCarmine, G. L. Gibson, J. Hollinger, L. M. Kozycz and D. S. Seferos, *Macromolecules*, 2013, **46**, 3879–3886.

43 C. X. Cui and M. Kertesz, *Phys. Rev. B.*, 1989, **40**, 9661.

44 C. Roux, J.-Y. Bergeron and M. Leclerc, *Macromol. Chem.*, 1993, **194**, 869–877.

45 C.-G. Zhan, J. A. Nichols and D. A. Dixon, *J. Phys. Chem. A.*, 2003, **107**, 4184–4195.

46 M. Dubois, S. Latil, L. Scifo, B. Grévin and A. Rubio, *J. Chem. Phys.*, 2006, **125**, 034708.

47 H. Zhou, L. Yang and W. You, *Macromolecules*, 2012, **45**, 607−632.

48 B. G. Zhao, Y. He and Y. Li, *Adv. Mater.*, 2010, **22**, 4355–4358.

49 M. G. Murali, Ar. D. Rao, S. Yadav and P. C. Ramamurthy, *Polym. Chem.,* 2015,**6**, 962-972.

50 F.C. Spano, C. Silva, *Annu. Rev. Phys. Chem.,* 2014, **65**, 477–500.

51 M. Böckmann, T. Schemme, D. H. de Jong, C. Denz, A. Heuer, N. L. Doltsinis, *Phys. Chem. Chem. Phys.,* 2015, **17**, 28616–28625.

52 W. C. Tsoi, D. T. James, J. S. Kim, P. G. Nicholson, C. E. Murphy, D. D. C. Bradley, J. Nelson and J.-S. Kim, *J. Am. Chem. Soc.*, 2011, **133**, 9834–9843.

53 A. Milani,L. Brambilla, M. Del Zoppo, G. Zerbi,*J. Phys. Chem. B.,* 2007, **111**, 1271–1276.

54 A. P. Scott and L. Radom, *J. Phys. Chem.*, 1996, **100**, 16502–16513.

55 A. Baggioli, and A. Famulari, *Phys. Chem. Chem. Phys.*, 2014, **16**, 3983-3994.

56 W. Yu, J. Zhou and A. E. Bragg, *J. Phys. Chem. Lett.*, 2012, **3**, 1321–1328.

57 L. Brambilla, M. Tommasini, I. Botiz, K. Rahimi, J. O. Agumba, N. Stingelin and G. Zerbi, *Macromolecules*, 2014, **47**, 6730-6739.

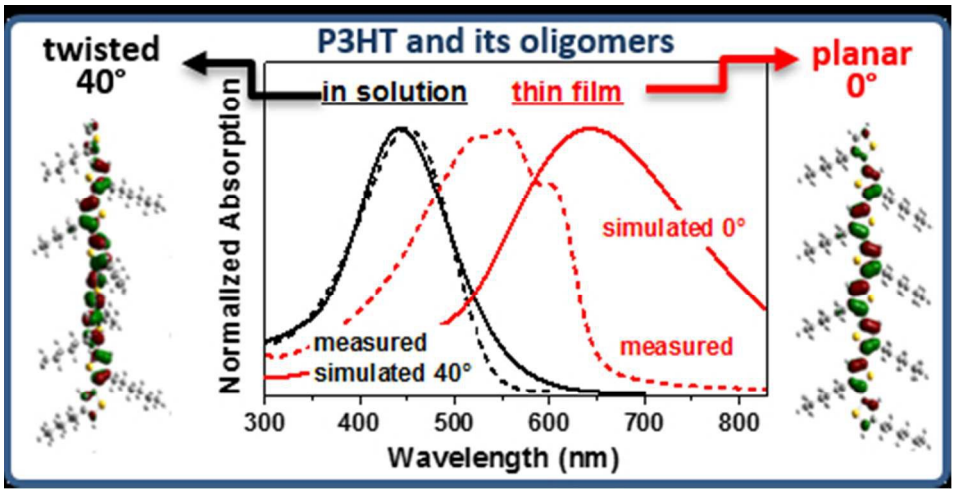

80x40mm (150 x 150 DPI)